



## Distribution and fate of trawling-induced suspension of sediments in a marine protected area

Torsten Linders<sup>1\*</sup>, Per Nilsson<sup>2</sup>, Andreas Wikström<sup>3</sup>, and Mattias Sköld<sup>3</sup>

<sup>1</sup>Department of Marine Sciences, University of Gothenburg, Box 461, S-405 30 Gothenburg, Sweden

<sup>2</sup>Department of Marine Sciences, University of Gothenburg, 452 96 Strömstad, Sweden

<sup>3</sup>Department of Aquatic Resources, Institute of Marine Research, Swedish University of Agricultural Science, Turistgatan 5, S-453 30 Lysekil, Sweden

\*Corresponding author: tel: +46 31 7862873; fax: +46 31 7862560; e-mail: [torsten.linders@marine.gu.se](mailto:torsten.linders@marine.gu.se)

Linders, T., Nilsson, P., Wikström, A., and Sköld, M. Distribution and fate of trawling-induced suspension of sediments in a marine protected area. – ICES Journal of Marine Science, doi:10.1093/icesjms/fsx196.

Received 10 July 2017; revised 28 September 2017; accepted 29 September 2017.

Bottom trawls suspend sediments by physical contact and the drag created by the gear when towed over the seafloor. Increased turbidity and redistribution of sediments may be of concern as some organisms are vulnerable to increased levels of sediment particles in the water column. This study investigates the distribution and fate of trawling-induced suspension of sediments in a coastal marine protected area (MPA). Bottom trawling is allowed in a deep trench of the MPA and regulated to weekdays with weekend closures. We use the closed period as controls to experimentally investigate sediment resuspension generated by the trawling fleet. We find that the turbidity is elevated at trawled depths and originates from small particles of silt–mud seafloor origin that remain suspended for days preventing background levels to be reached during closures. Peaks in the plumes behind trawlers reach levels critical to organisms but decays within hours. Currents in the trench are too weak to resuspend sediments; however, wind-induced resuspension events of elevated turbidity likely originating from nearby shallower areas may occur. Short-term closures and small-scale MPAs are concluded to be of limited use as management tools to reduce effects of resuspension by bottom trawling.

**Keywords:** fishery management, MPA, otter trawling, *Pandalus borealis*, resuspension trawling, turbidity.

### Introduction

Sediments are built up over geological time scales by accumulation of particles of physical, chemical and biological origin and the result of complex particle histories involving processes, such as mineralization, bioturbation, deposition, resuspension, and transport (Hall, 1994; Lynch *et al.*, 2015). Sediment particles are to various extent mobile depending on size, shape, and density (Newton and Liss, 1990). Natural resuspension of sediments by hydrodynamics (wind and currents) may differ substantially on short spatial scales from being essentially absent on deeper soft bottoms to constant in the exposed photic zone. Severe storms may induce resuspension at depths down to 130 m as recorded by Sherwood *et al.* (1994) on the exposed Californian coast, but rarely below 50–70 m as described by Danielsson *et al.* (2007) for the open Baltic proper. Anthropogenic processes may interact as

well with sedimentation and the transport of particles, either by dredging for ship routes and constructions, or by exerting energy e.g. from the propulsion of boats or by fishing operations. Comparing natural disturbance of the seafloor with disturbance to the sediment from fisheries in the North Sea and the Baltic show that the fishing impact largely exceeds natural disturbance in muddy substrates and deep circalittoral habitats (Floderus and Pihl, 1990; Diesing *et al.*, 2013; Martín *et al.*, 2014a; Tjensvoll, 2014).

Bottom trawling is a fishing activity that impacts the seafloor and even has the capacity to modify the seafloor morphology and sedimentary regimes (Puig *et al.*, 2012; Martín *et al.* 2014b; Oberle *et al.* 2016; Paradis *et al.*, 2017). The impact is created by those parts of the gear that are in direct physical contact with the bottom during the operation, and by the hydrodynamic drag of

the gear over the bottom, which suspend large volumes of sediments up in the water column (e.g. O'Neill and Summerbell, 2011; Bradshaw *et al.*, 2012; Depestele *et al.*, 2016). These processes increase near bottom turbidity and may result in significant transport of sediment to deeper areas via erosion of recent sediments (Churchill, 1989; Churchill *et al.* 1994; Martín *et al.*, 2014c), and sediment gravity flows (Palanques *et al.*, 2006). Trawling-induced resuspension of accumulated sediments may also reduce the organic content of the surface layer (Puscieddu

*et al.*, 2014), and contribute to the mobilization of nutrients (Dounas *et al.*, 2007) and contaminants (Bradshaw *et al.*, 2012). Increased suspension of sediment and elevated turbidity may also have ecological impact on organisms due to reduction of light affecting primary producers in shallow waters (Moore *et al.*, 1997), and increase mortality of egg and larvae of fish and invertebrates (Westerberg *et al.*, 1996; Gilmour, 1999). Suspension feeders such as mussels and sponges are selective feeders and depend on organic particles in the bottom water. Relative changes in the

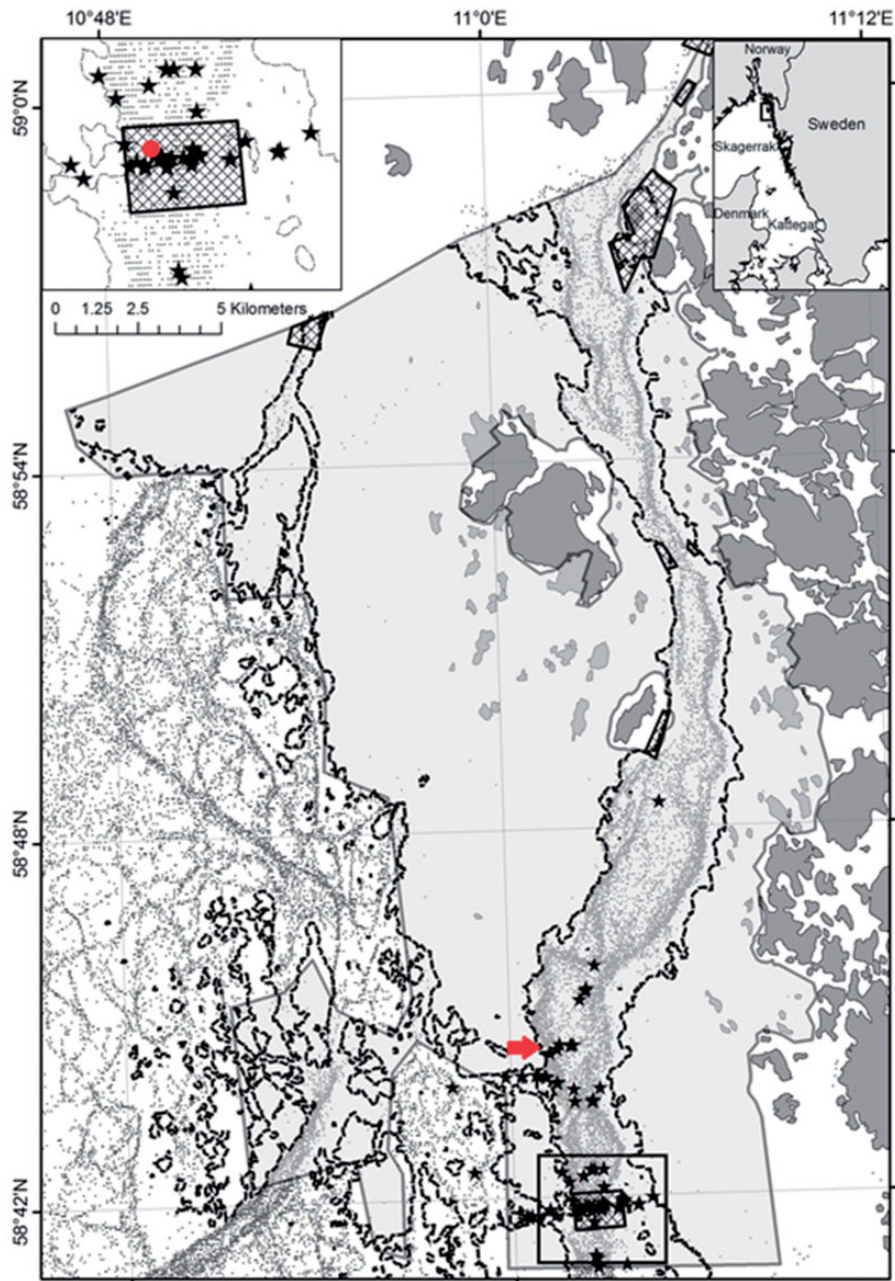


**Figure 1.** Map of the study area. The KNP is indicated in light grey and SPAs within the park are crosshatched polygons. Small black dots are satellite positions (hourly VMS pings) of active bottom trawlers 2012–2014. The upper trawling limit at 60 m depth is indicated by the stitched line. The large region with no trawling activity is mainly shallower than 60 m. Stars show position of all casts measuring turbidity. The red circle inside the SPA in the inset of the upper left corner of the figure indicates where instruments were moored in October 2012. The red arrow points to the positions of the measurements after the passage of two trawlers. Colour version of this figure is available online.

quality and size of particles due to resuspension of sediments may thus affect feeding and oxygen consumption (Johnston and Wildish, 1982; Tjensvoll *et al.*, 2013; Kutti *et al.*, 2015). Fish may also be sensitive to increased levels of fine particles due to clogging of gills (Humborstad *et al.*, 2006).

In shelf and coastal ecosystems a mixture of habitats are common where reefs, sand banks, and shallow areas with vegetation border deeper areas like submarine canyons, trenches and plains with soft sediment bottoms. In these heterogeneous areas biodiversity is high as one habitat with its communities borders the next and the connections of biological and physical processes between habitats are strong. Marine protected areas (MPAs) is one way of managing biodiversity and often involves zonation of activities to allow for use of part of areas as long as conservation targets are not jeopardized (Bergström *et al.*, 2016). Establishing restriction zones are theoretically a straightforward measure to protect core values in an MPA from direct physical impact from trawl fisheries. However, designing zones to protect against the indirect disturbance from increased turbidity due to resuspension in the bottom water is less obvious due to the usually small scale, and the heterogeneity of the habitats and the benthic pelagic coupling that may occur within a coastal MPA.

The aim of this study is to describe the temporal and spatial distribution, evolution, and fate of sediment particles resuspended by bottom trawling. The study shows vertical distribution of turbidity and associated particle composition, and that background levels at trawled depths are increased during weekly trawling activities in a coastal MPA. The results are discussed in perspective of the conservation targets and the potential for management of trawling-induced resuspension of sediments in MPAs.

## Methods

### Study area

Figure 1 shows the Koster Sea on the west coast of Sweden, with location map showing the area around Skagerrak and Kattegat. The brackish Baltic Current follows the Swedish coast, in Skagerrak forming a low saline wedge extending about 10 km from the coast (Rodhe, 1998), with surface layer salinity typically 24–27 PSU. The tidal regime is semidiurnal, with amplitude around 10 cm (Svansson, 1975). Charts of seasonal maximum sea ice cover for the region show that extensive sea ice is very rare in the Koster Sea (SMHI, 2017). The surface circulation is wind driven (Aure and Saetre, 1981), with freshwater accumulating in the north eastern Skagerrak during south westerly or westerly winds (Gustafsson and Stigebrandt, 1996). The surface layer when the wind slackens or changes direction (Aure and Saetre, 1981). In a north–south direction, to the east of the Koster Isles, runs the Koster trench, with a maximum depth of 247 m. The trench has steep sides, typically sloping downwards from 60 m and is divided into several deep basins separated by sills to the south with depths around 70 m. The north end of the trench has a deeper sill (110 m) and is more open to the deeper parts of the Skagerrak. The basin water of the trench has relatively stable characteristics revealing its Atlantic origin, typically with salinity above 34.2 PSU and temperature below 8 °C. Ventilation of the trench occurs during surface layer outbreaks and the accompanying upwelling of denser water masses.

The Kosterhavet National Park (KNP) is an MPA where multiple uses are allowed. The most important fishery in the KNP is bottom trawling for northern prawn *Pandalus borealis*, landing around

150 tonnes of prawn yearly. The trawl gears used by the fleet are diamond mesh trawls ( $\geq 35$  mm mesh opening). The ground gear of the net is equipped with bobbins and is regulated in size [maximum 50 m wide and weight of the otter boards 350 kg and surface area 2.7 m<sup>2</sup> (SwAM, 2004)]. The trawl fishery is licensed and allowed only in areas below 60 m depth, which is mainly the central deep trench of the KNP. To further safeguard certain areas below 60 m with high biodiversity, e.g. sponge and seapen communities and deep water coral reefs of *Lophelia pertusa*, small seabed protection areas (SPAs) where trawling is prohibited have been established, marked with crosshatched polygons in Figure 1. The prawn fishermen have also initially voluntarily established Friday to Sunday closures. However, new regulations for prawn in the MPA were adopted in July 2015. The updated regulations states that fishing is only allowed three days per week and only during weekdays from 05.00 to 20.00 resulting in week end closures.

### Experimental procedures

The main experimental set-up of the study is to compare turbidity during a day at the end of the voluntary closures, with turbidity during a day of trawling activity in the KNP. The experiment was repeated five times, each time with two survey days and each day with approximately 20 vertical profiles, using standard rosette samplers equipped with a CTD and turbidity sensor. Most, but not all, of the stations were revisited during the five experiments. All of the five experiments cover exclusively the same basins and depths of the trench. In order to get a detailed characterization of a trawl plume targeted profiling in a temporal sequence was also measured immediately behind two trawlers at one survey.

During one of the experiments (October 2015, both of the survey days) turbidity and water quality was resolved in the same way by water sampling measuring total suspended mass. Laser *In Situ* Scattering and Transmissiometry (LISST) was also used during the same experiment to study suspended particle volume concentrations and particle size distributions.

To further study the continuous variation in turbidity, currents and the dispersal potential of suspended matter, instruments were moored during 15 days in one of the small SPAs in the middle of the trawled trench of the KNP. The mooring consisted of a CTD fitted with turbidity sensor and an Acoustic Doppler Current Profiler (ADCP).

### Measurements and sample processing

Table 1 summarizes our measurements. Vertical profiling was conducted from either R/V Nereus or R/V Skagerak in five experiments. The positions of all profiles are shown in Figure 1. The profiling were made with a rosette water sampler fitted with a CTD (SBE 19plus v2 on R/V Nereus, SBE 9 on R/V Skagerak) and a turbidity sensor (WET Labs ECO-NTU, range 0–125 NTU, on R/V Nereus; WET Labs ECO-FLNTU, range 0–25 NTU, on R/V Skagerak). The detailed measurements of trawl plumes immediately behind trawlers on 1 April 2014, were made with a microstructure profiler (ISW Wassermesstechnik) fitted with a Seapoint turbidity sensor (range 0–25 FTU). The microstructure profiler is designed for freely sinking measurements all the way to the bottom, the primary parameter being turbulence calculated from micro-shear sensors, but sensors for other parameters (e.g. turbidity) can also be fitted. The two different turbidity sensors (WET Labs and Seapoint) and turbidity units (NTU and FTU) are approximately the same. Both measure side scatter of



**Table 1.** Summary of measurements.

Periods	Vertical profiling with turbidity sensor	Mooring with turbidity sensor and ADCP	Vertical profiling with LISST
Sunday 26 and Monday 27 August 2012	X	–	–
Thursday 4– Friday 19 October 2012	–	X (both closed and trawled periods)	–
Friday 5 and Thursday 18 October 2012	X	–	–
Wednesday 1 April 2014	X (behind trawlers)	–	–
Sunday 19 and Monday 20 October 2014	X	–	–
Sunday 3 and Monday 4 May 2015	X	–	–
Sunday 4 and Monday 5 October 2015	X	–	X

emitted light (700 nm for WET labs and 880 nm for Seapoint) and both use Formazin as a calibration standard. Hongve and Åkesson (1998) report that sensors using  $860 \pm 10$  nm (ISO 7027) typically generate about 10% higher values than sensors using 400–600 nm wavelengths. Turbidity is typically used (as in our study) as a proxy for particulate matter. The shorter wavelengths are partly influenced by coloured dissolved matter.

To estimate total suspended matter (TSM), water samples were taken using Niskin bottles (10 l) in parallel with the profiling on 3–4 May 2015. The samples were taken close to the bottom at 60–186 m depths with the aim to cover the range of near bottom turbidity shown in the turbidity profiles. TSM was determined by filtering 2 l of seawater on rinsed, burned (500 °C) pre-weighed glass fibre filters (GF/F 0.7  $\mu$ m). Filters were weighed after 3 days at 60 °C to the nearest 0.00001 g.

To measure particle volume concentrations and particle size distributions a LISST-100X (Sequoia Scientific) was mounted on the rosette water sampler. The laser diffraction method determines the size distribution of particles by recording the scattering intensity of particles, which can be converted into volume concentrations of particles in 32 logarithmically increasing size ranges between 2.5–500  $\mu$ m (Agrawal and Pottsmith, 2000). Measurements were taken in parallel with the profiling on 4–5 October 2015.

On 4 October 2012, instruments were moored inside the SPA marked in Figure 1. The instruments were a CTD (SBE 19plus v2), turbidity sensor (WET Labs, ECO-NTU, range 0–125 NTU) and an ADCP (300 kHz, RDI Teledyne WorkHorse). The CTD were placed 1 m above the bottom (at 98 m depth) and logging once each minute. The ADCP were placed 0.5 m above the bottom (at 93 m depth), with a 6-s pinging interval and averaging over 2 min. ADCP data were put into 2-m-depth bins, with the lowest bin starting  $\sim$ 4 m above the bottom. The instruments were moored in close proximity at the western side of the trench (position marked with a red circle in the small inlet of the upper left corner of Figure 1) and were retrieved after 15 days.

Trawling activity was evaluated using logbooks and the Vessel Monitoring Systems (VMSs). The Swedish logbook includes gear set positions, which was used to estimate fleet composition and size of vessels in the KNP. Mean size of vessel engine power was 263 kW. About 76% of the vessels were equipped with a VMS transmitter providing information on identity, position, time, course and speed approximately every hour to a satellite-based information system (Inmarsat-C). Periods of fishing activity were assigned to vessel and gear type by linking the VMS data to the logbook using the vessel identifier and time. Instantaneous speed was used to determine the occurrence of a fishing event. Inspection of vessel speed distribution suggested trawling speed between 1.25 and 2.25 knots, and the data were filtered

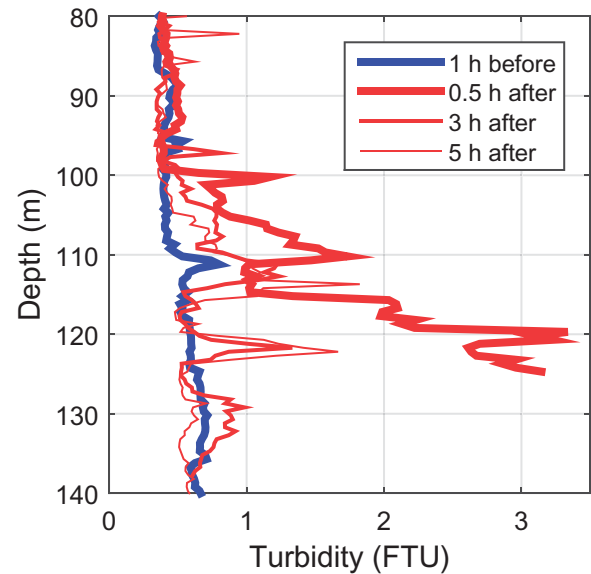


**Figure 2.** Vertical profiles of turbidity before and after the passage of two trawlers. The profiles after the passage were sampled in close proximity to where the two trawlers met, coming from opposite directions and passing only some hundred metres from each other. Colour version of this figure is available online.

accordingly (Gerritsen and Lordan, 2011). Periods of trawling activity were cross-checked with the logbook gear set positions to verify presence of smaller trawlers not equipped with VMS.

### Statistical analyses

To evaluate the effect of trawling, turbidity was analysed using a two-factorial ANOVA with trawling/non-trawling as a fixed factor and experimental day as random factor. Testing was performed by profiles for three separate depth intervals being above allowed trawling depths (<60 m), within trawling depths (60–150 m), and deeper, trawled depths (>150 m). Within each profile average turbidity and coefficient of variation for all measurements within each depth interval was calculated. Visual inspection of residual plots showed that a common pattern in the datasets was that there was a relationship between mean and variance, which means that the distribution of data was not normally distributed and that variances were heterogeneous. In such cases, data were  $\ln(x + 1)$  transformed before statistical testing to normalize data and make variances more homogenous. Analyses were performed using the software R version 3.1.3 and the program library Imer4 and ImerTest for analysis of variance with Type III-Sum of Squares.

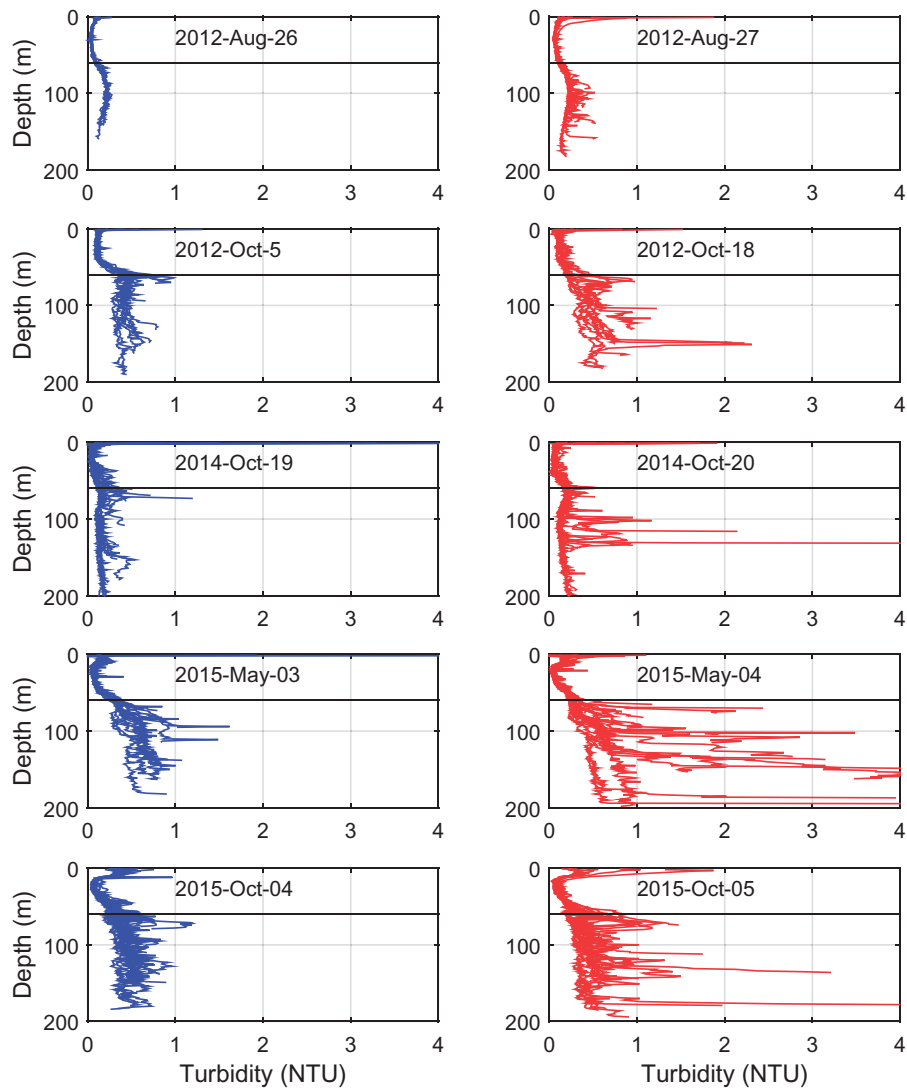


**Figure 3.** Pairwise comparison of vertical profiles of turbidity in KNP during closed days (left panels, blue lines) and trawled days (right panels, red lines). Black solid lines at 60 m depth mark upper limit allowed for trawling. Colour version of this figure is available online.

Frequency analysis of the turbidity measurements from the mooring was performed by a fast Fourier transform algorithm, using the software Matlab (R2014b).

Linear regression was used to analyse the correlation between turbidity and TSM.

### Estimating horizontal transport

The sinking velocity,  $w_s$ , of a particle can be calculated from its diameter and its density using Stoke's law (e.g. Kundu and Cohen, 2002). We assume that the suspended particles have a density  $2600 \text{ kg m}^{-3}$ , i.e. proxy for quartz. While sinking, the particles will be transported a horizontal distance,  $\delta x$ , depending on the average horizontal flow,  $u$ , of the water in the path of the sinking particles. If  $\delta z$  is the particle's initial vertical displacement above the bottom, then

$$\delta x = \delta z \frac{u}{w_s}. \quad (1)$$

## Results

### Estimating height and width of a trawling-induced plume

On 1 April 2014, measurements were conducted after the passage of two trawlers. The location was on the western slope of the trench around latitude  $58^\circ 45' \text{ N}$ , see red arrow in Figure 1. The two trawlers were coming from opposite directions, following the side of the trench. Figure 2 shows the temporal change of the turbidity after the passage of the trawlers around the depths of trawling. For comparison the figure shows one profile with measurements inside the SPA 5 km to the south,  $\sim 1 \text{ h}$  before the earlier. The other three profiles show measurements in close vicinity of the passage,  $\sim 0.5$ ,  $2.5$ , and  $5 \text{ h}$  after the passage. The profiles are on the sloping side of the trench, with the  $0.5 \text{ h}$  profile furthest upslope, to the west. Based on their positions, the bathymetry and the peaks in turbidity we estimate that the two trawlers had their gears at around 110 and 120 m depth, respectively.

The measurements 0.5 h after the passage show turbidity levels elevated to 1–2.5 FTU, over a depth interval 100–125 m. The following measurements, 3 and 5 h after the passage, indicate the decay of the plume, with lowering turbidity. We assume that the 25 m thick layer of elevated turbidity comes from the passage of two trawls at different depths. From this we conclude that an initial trawling plume in KNP is around 10 m in height. Based on the regulations of the maximum opening width of the trawl net (50 m) and consultation with local fishermen operating in the KNP that use sensors on the trawl doors, the spread between the trawl doors was measured to be around 42 m at fishing speed. Accordingly, we estimate that the door spread equals the initial plume of resuspended sediment and will be around 42 m in width.

**Table 2.** Trawling activity during 1–19 October 2012.

	Trawled				Closed		
	Monday	Tuesday	Wednesday	Thursday	Friday	Saturday	Sunday
<b>Date</b>	1	2	3	4	5	6	7
<b>VMS</b>	8	20	1	18	0	0	0
<b>Date</b>	8	9	10	11	12	13	14
<b>VMS</b>	5	0/X	21	9	0	0	0
<b>Date</b>	15	16	17	18	19	–	–
<b>VMS</b>	87	42	0/X	26	0	–	–

Each VMS recording represents ~1 h of trawling. The 5th and the 17th are crossed, because there was no trawling on these days due to strong wind.

### Vertical profiles of turbidity and particles—closed vs. trawling days

The logbook and the VMS database verified the weekend closures for the periods investigated. Sundays were thus confirmed as control days without trawling influence 72 h prior to measurements. However, the control day 5 October 2012, is an exception being a Friday with the last trawling activity in the KNP the day (ca. 17 h) before measurements were taken. The left hand panels in Figure 3 show vertical background profiles for control days without trawling. The surface layer may have high turbidity peaks, decreasing to lowest levels (0.05–0.2 NTU) around 15–35 m depth. The turbidity then increases slightly to around 0.2–0.7 NTU below 60 m, i.e. the depth where trawling is allowed. A few peak values above 1 and 1.5 NTU are observed. There is homogeneity in the data at a given depth between measurements during the same day which indicates strong horizontal similarity of the water layers. However, the variation in background turbidity varies considerably between periods as indicated by the difference between the control days.

The right-hand panels of Figure 3 show vertical profiles for days with trawling. This allows for pairwise comparisons of control vs. trawled days for the five profiling experiments conducted in the study. In the results there are pairwise similarities between the turbidity profiles of the control days and of the corresponding trawled days. The statistical tests comparing trawled with control days show significant increased average turbidity ( $F_{1,4} = 8.35$ ,  $p = 0.044$ ), and higher coefficient of variation, CV ( $F_{1,4} = 13.47$ ,  $p = 0.022$ ) in the 60–150 m depth interval where trawling is

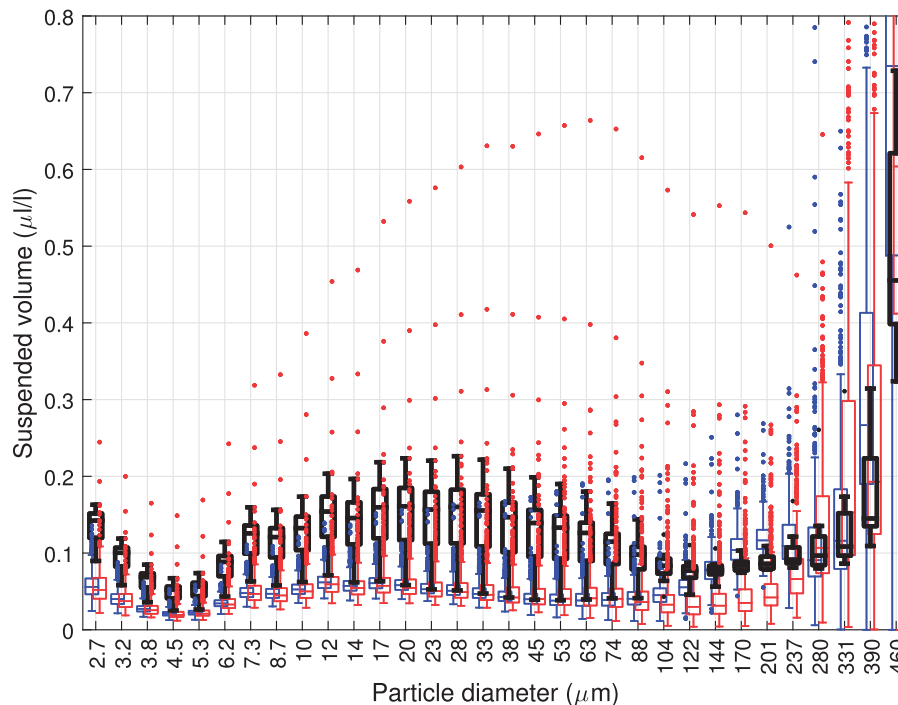


**Figure 4.** Boxplot of particle size distribution measured with LISST. The data are from the trawled depth interval 60–150 m on 4th October (closed, blue in graph) and 5th (trawling, red in graph), 2015. Black are data from a single profile in the depth interval 130–146 m on the 5th, behind a trawler. The central mark of each box is the median, the edges of the box are the 25th and 75th percentiles and the whiskers extend to the adjacent values. The (maximum) length of the whiskers is 1.5 times the difference between the 25th and 75th percentiles. The remainder of the data are considered outliers and are marked with dots. Note how the black boxes and whiskers (for particles < 120 µm) largely cover the red outliers. Colour version of this figure is available online.

allowed. No differences were found in the non-trawled shallow depth interval 0–60 m (mean  $F_{1,4} = 0.72$ ,  $p = 0.44$ ,  $CV F_{1,4} = 5.72$ ,  $p = 0.075$ ), nor in the deepest depth interval >150 m (mean  $F_{1,3} = 2.37$ ,  $p = 0.22$ ,  $CV F_{1,3} = 6.85$ ,  $p = 0.079$ ). As mentioned earlier, the background turbidity regimes vary significantly between periods at all depth interval in both average turbidity and CV for turbidity ( $p < 0.05$ ).

TSM was strongly correlated to turbidity, and was characterized by the relationship  $TSM [mg \text{ dry weight (DW)} l^{-1}] = 1.225 \times \text{turbidity (NTU)} + 0.3556$ , with  $R^2 = 0.84$ . Based on measured turbidity levels TSM background levels were estimated to be within the range 0.5–1.6  $mg l^{-1}$  with occasional levels of 2.4  $mg l^{-1}$ . During trawled days levels are increased and within the range 0.8–4  $mg l^{-1}$ , and occasional high levels up to 5.8  $mg l^{-1}$ .

### Suspended particle size and volume

Volume concentration measurements per particle size interval measured by the LISST-100X were collected during 4 and 5 October 2015 being control and trawled days respectively. The effect of trawling on the size distribution is seen in the variation expressed as main distribution and outliers within the trawled depth interval 60–150 m (Figure 4, see caption for definition of outliers). On both days there is considerable spread in the main distribution and also numerous outliers. For size range up to around 120  $\mu m$  there are more high value outliers on the trawled day (red) compared with the control day (blue). Particles larger than 120  $\mu m$  generally have larger variation between profiles and show no clear patterns. The data marked with black in Figure 4 show measurements from one individual profile at trawled depths 130–146 m, taken behind a trawler on 5 October 2015. They are included and overlaid the averaged distribution in order to resolve the contribution from particles resuspended by trawling. For size range up to around 120  $\mu m$ , the distribution (with very few outliers) of this latter data captures well the high

value outliers from the same day (red dots in Figure 4). This indicates that those high value outliers on the trawled day correspond well with the main distribution of measurements inside a trawl plume, and are indeed likely caused by resuspension from trawling.

### Trawling activity and turbidity measurements from moored instruments

Table 2 shows the trawling activity divided into days during the period 1–19 October, 2012, when the moored instruments (ADCP and CTD with turbidity sensor) were deployed. As expected, trawling activity ceased during the weekends, however, trawling was as well absent from the fjord on the 9th and the 17th as the fleet stayed in port due to gale-force winds. At Väderöarna Islands, 15 km south of the moored instruments, it was observed 3.7 m significant wave height on the 17th, the highest of the month.

Prevailing currents were strongest in the north–south direction and the magnitudes were in general  $< 0.2 m s^{-1}$  (Figure 5). Below 70 m the magnitudes decreased slightly, with the exception of one event on the ninth with  $0.2 m s^{-1}$  easterly current reaching down to 80 m depth. Only above 50 m there were signs of semidiurnal tide, e.g. visible as alternating east–west currents on the 10th and 11th (Figure 5, top panel). The diel pattern with gaps in the data above 20 m in Figure 6 is likely caused by migrating zooplankton (Bengt Liljebladh, personal communication). Many investigations have shown that zooplankton migration can be traced in ADCP data (e.g. Liljebladh and Thomasson, 2001; Rippeth and Simpson, 1998; Heywood et al., 1991), although we have found no similar example of gaps in data. Below 70 m there were slanting bands visible in the north velocity, most clearly during the 13th indicating internal waves generating currents propagating upwards. The magnitude of currents below 70 m was mostly between 0 and  $0.05 m s^{-1}$  and especially for the depth interval below 80 m there were very few instances with

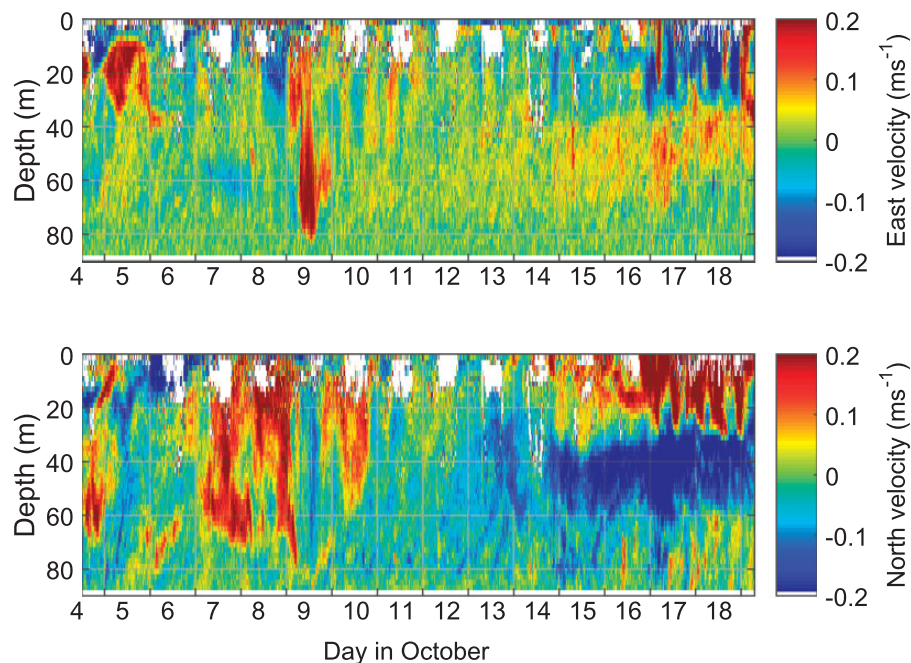


**Figure 5.** Velocities from the moored ADCP, east (top) and north (bottom). Colour version of this figure is available online.



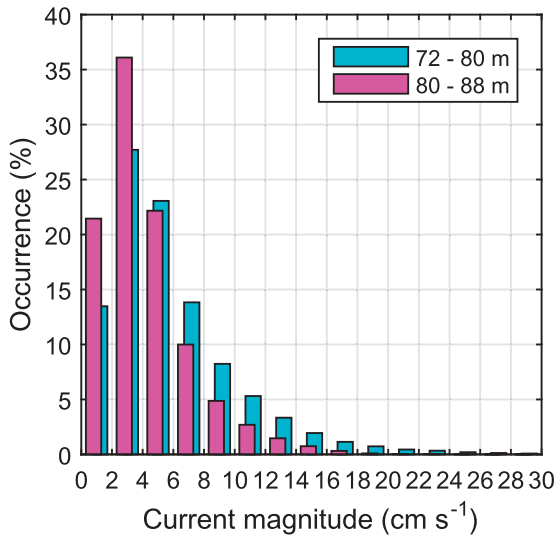


**Figure 6.** Histogram of velocity magnitudes from moored ADCP. The data are all (2 min) ensemble averages from the entire deployment of the two deepest 8-m-depth intervals. Colour version of this figure is available online.

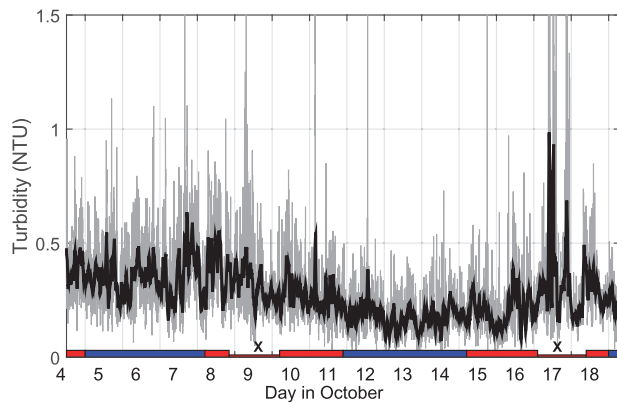


**Figure 7.** Instant turbidity (thin grey) and 1-h average turbidity (thick black). Colour bar at the bottom indicate trawled periods (red) and closed periods (blue). Periods with no trawling due to strong wind are crossed. Confer Table 2. Colour version of this figure is available online.

magnitudes above  $0.1 \text{ m s}^{-1}$  (Figure 6). From this we conclude that  $0.04 \text{ m s}^{-1}$  is a reasonable value for estimating the horizontal transport of resuspended particles. Which magnitudes that are required to erode and resuspend sediments is a nontrivial question. Controlling factors include not only particle size but also resuspension history (Churchill et al., 1994). However, the magnitudes we measure in the Koster trench are typically not sufficient to cause resuspension.

The instant turbidity was variable with short events of elevated turbidity (<3 min and >3 NTU, grey line in Figure 7). The days 9 and 17 October (marked as crossed in Figure 7) indicate when gale force winds occur and the fleet stay in port. On 17 October, coinciding with gale force wind, there were a total of 24 measurements above 1.5 NTU with a 7-min event of up to 7.5 NTU and 1-h average turbidity reaching 1 NTU (black line in Figure 7). The events with high values on the 17th were thus strong enough

**Table 3.** Approximate sinking velocity, sinking time and horizontal transport for particles displaced 10 m above the bottom in a horizontal flow speed  $4 \text{ cm s}^{-1}$ .

Class	Size (mm)	Velocity ( $\text{mm s}^{-1}$ )	Time	Transport
Clay and silt (very fine)	<0.005	>0.014	>8 days	>28 km
Silt (fine)	0.01	0.057	2 days	7 km
Silt (medium)	0.02	0.23	12 h	1.7 km
Silt (coarse)	0.05	1.4	2 h	280 m
Sand (very fine)	0.1	5.7	29 min	70 m
Sand (fine)	0.2	23	7 min	17 m

Size classes are according to Wentworth (1922). The sinking velocity is calculated from Stoke's law (see "Dispersal and fate of suspended particles" section).

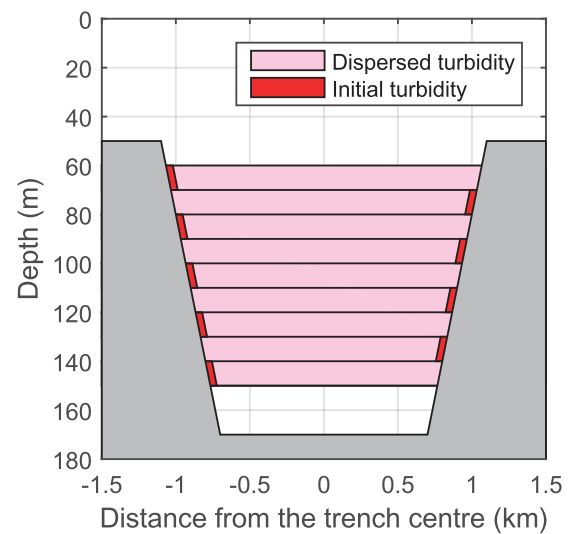


**Figure 8.** Schematic illustration of dispersion across the trench. The initial turbidity is assumed to come from 10-m-high and 42-m-wide plumes caused by trawling along the slopes of the trench. Colour version of this figure is available online.

to significantly influence the 1 h average. Although the mean of hourly turbidity values on the gale day 9 October do not differ significantly (ANOVA  $F_{1,94} = 1.47$ ,  $p = 0.283$ ) from other days within the same fishing period 8–11 October, the mean hourly values on the gale 17th is significantly higher (ANOVA  $F_{1,94} = 25.4$ ,  $p < 0.001$ ) than the mean hourly values of other days during that fishing period (15–18 October). The elevated turbidity associated to the gale on the 17th showed that wind episodes may generate increased turbidity in the trench down to at least 98 m depth where the turbidity sensor was moored, thus masking the turbidity signals from trawling. A frequency analysis indicates that the variability is distributed over a very broad range of frequencies, with no peak around the tidal frequency.

The 1-h average turbidity was significantly (ANOVA  $F_{1,354} = 4.13$ ,  $p = 0.043$ ) higher during periods open for trawling ( $0.278 \pm 0.015$ ) than during closed periods ( $0.264 \pm 0.017$ ). However, this comparison is confounded by the two gale events that occurred on 9 and 17 October, both days potentially open for trawling. If data from these two days are excluded from the analysis, there is still a higher average turbidity during trawl days ( $0.272 \pm 0.004$ ) than



during closed days ( $0.264 \pm 0.011$ ), but this difference is not statistically significant (ANOVA  $p = 0.47$ ).

The 1-h average turbidity decreased slightly with time during closed periods, but this correlation was not statistically significant (Pearson correlation coefficient  $r = -0.052$ ,  $p = 0.53$ ). However, the 1-h average turbidity increased significantly with time after trawling was resumed (Pearson correlation coefficient  $r = -0.356$ ,  $p = 0.006$ ). The latter analysis may however be confounded by the storm events, when trawling was stopped. If the data for the days 9 and 17 October are excluded from the analysis, the positive correlation between turbidity and time since trawling was resumed is somewhat lower, but still significant (Pearson correlation  $r = 0.256$ ;  $p = 0.001$ ). However, this significant correlation is then strongly influenced by some data points, which is shown by the fact that the correlation is not statistically significant if a Kendall nonparametric rank correlation test is used instead ( $p = 0.27$ ).

### Dispersal and fate of suspended particles

Table 3 shows the sinking time and horizontal transport (see “Estimating horizontal transport” section) for particles of different sizes classes given that:

- (i) trawling causes vertical displacement  $\delta z = 10$  m. This is the upper limit of the trawl plume (see “Estimating height and width of a trawling-induced plume” section);
- (ii) the average flow is  $u = 0.04$  m s<sup>-1</sup> (see “Trawling activity and turbidity measurements from moored instruments” section).

Particle size has a large influence on the horizontal transport of resuspended particles, see column “Transport” in Table 3. Sand will typically be transported only a distance in the range of 10–100 m. The finer fractions of clay and silt, on the other hand, may remain in suspension long enough to be transported distances comparable to the length of the basins in the Koster trench, or longer. Coarse and medium silt fall somewhere in between these two categories.

The sides of the Koster trench slope relatively constantly down to about 150 m. The trawling activity is also relatively even along the sides of the trench (Figure 1). This allows us to treat the trench ~2-dimensionally. For the small particles, being resuspended into the water column by trawling, the relevant dispersal process will be advection across the trench. Figure 8 shows this schematically. This simplified model could explain why the turbidity is higher at typical trawling depths, even after a closure of several days (left panels in Figure 3).

### Discussion

We have measured turbidity in KNP on the west coast of Sweden. The measurements were conducted as vertical profiling, both inside a trawling prohibited SPA and in other parts of the Koster trench, where trawling is allowed. In addition we have moored logging instruments, and measured turbidity and velocity for a 2-week period. The vertical profiles show that the average turbidity is about 12% higher on the days of trawling compared with periods of closure. The higher average comes from occurrences of layers where the turbidity is several times higher than the background levels. The continuous measurements from moored instruments support this pattern, since the average turbidity

increase when trawling is resumed after the closures. The continuous measurements also show that natural events, such as strong gales, largely mask the effect on turbidity from trawling.

The fate of resuspended particles is governed by particle size and density, and by the strength of the water flow that transports the particles. The largest particles will tend to settle in the vicinity of the trawling tracks. The finest size fraction will sink so slowly that other processes like being ventilated out of the area are more important than gravitational settling. The theoretical framework is based on ideal spherical shapes with particle density similar to quartz, and uses size as a proxy for post-glacial sediment particles. In reality marine aggregates do not conform to this and are usually lighter and not spherical and thus having significantly slower sinking speed than idealised particles (Allredge and Gotschalk, 1988). Our framework thus likely overestimates the sinking speed of the large fraction of the particles.

The dominant suspended particle size volume causing the increased turbidity in the KNP is between 2 and 120  $\mu\text{m}$ . This corresponds to the typical postglacial silt–clay sediments dominating the seafloor of the deeper basins of the KNP as well as vast soft seafloor areas along the Swedish coast (Cato, 2006; Klingberg, 2015). During each of our five experiments, with one closed survey day and one trawled survey day, we found similar average vertical profiles of increased turbidity at levels of the trawling depths. This is a strong indication that also part of the background turbidity is dominated by small particles, with negligible sinking speed originating partly from trawling-induced resuspension.

Martin *et al.* (2014a) also found that turbidity varied in relation to periods of trawling and measured lingering bottom and intermediate nepheloid layers with turbidity levels resembling what was observed in KNP. Their investigation took place along a flank of a deeper Mediterranean canyon and using moored systems they also detected high turbidity well below the working depths of the trawling fleet created by gravity flows.

The different fate of particle size categories has significant implications if the management concern is protection from suspended particles caused by nearby resuspension by trawling. For example, if the aim is to protect from deposition of large heavy particles, e.g. resuspension of sandy substrates, it may be sufficient with a limited safety distance in the range of 10–100 m. However, if the objective is protection from smaller particles it is likely not sufficient to increase the safety distance within an MPA, as that would need buffer zones at the scale of km or more that may well be larger than the MPA itself. It is thus important with knowledge about prevailing current regimes. If management objectives include protection from elevated turbidity caused by small particles it is not sufficient with safety distances at all. In the case of small particles with negligible sinking speed in relation to the horizontal transport, measures should instead target to balance the intensity of sediment disturbance from e.g. trawling activity by the efficiency of the water exchange of the area. A trawling plume in KNP may be up to 10 m high and 42 m wide, with turbidity elevated 1 NTU, or more in its peaks. The KNP trench is on average ~40 times as wide as the plume. Considering that the turbidity is mainly caused by small particles (clay—fine silt), dispersion of such a plume across the trench will yield a 10-m layer with turbidity elevated 0.025 NTU. Each time this trawling pattern is repeated the turbidity will increase 0.025 NTU in this layer. Trawling on four adjacent levels would create a 40 m thick layer with elevated turbidity. Repeating the trawling pattern eight times (at each level) would create a layer with turbidity elevated to 0.2 NTU, qualitatively resembling the

situation on e.g. 26 August 2012. A total of 32 trawl hauls would thus be sufficient to create the turbidity observed on one of our days of measurements.

A large number of particles are smaller than 0.005 mm and would thus not be deposited before next period of trawling. In other words, since closed periods are only around 84 h, and exchange of the water masses below sill depths is limited, it is likely that background turbidity is never reached in the trench of the KNP, which is supported by the vertical profiles indicating elevated turbidity at trawl depths (deeper than 60 m, see left panels in Figure 3) also at the end of closed periods.

Bradshaw *et al.* (2012) investigated the resuspension caused by trawling in Eidangerfjorden, southern Norway, which has similar fine silt–mud fjord sediments as the KNP. In that investigation, the volume concentration of suspended material was dominated by particles 0.01–0.03 mm 30–60 min after the passage of a trawler (Molvær *et al.*, 2012). The plume in the investigation by Bradshaw *et al.* (2012) is similar in turbidity range (1–5 NTU), but wider (120–150 m) and somewhat higher (15–18 m) compared with what we estimate for the trawls in KNP.

During days without trawling activity in KNP the concentration of suspended material measured in DW, ranged between 0.52 and 1.6 mg/l, with occasional peaks to maximum of 2.4 mg/l. In contrast, during days with trawling the concentration of suspended material ranged to 0.8–4 mg/l, with peaks up to 5.8 mg/l in the water mass. These elevated levels of suspended materials in the water mass during days with trawling in KNP may pose a risk to marine organisms since they exceed levels where effects have been documented (Westerberg *et al.*, 1996; Larsson *et al.*, 2013). In the study by Westerberg *et al.* (1996) an increased mortality of cod yolk-sack larvae during exposure of concentrations of 10 mg/l and avoidance behaviour for cod (*Gadus morhua*) and herring (*Clupea harengus*) during exposure of levels by ~3 mg/l was documented. Furthermore, in exposure of cod eggs to sediment suspensions also resulted in particles adhering to the surface of the eggs. This effect gave a loss of buoyancy which was proportional to the sediment concentration and the exposure time (Westerberg *et al.*, 1996). This means that the process can make the eggs sink to the bottom even at relatively low sediment concentrations. The authors raised a concern about this effect because; if an egg sinks to the bottom this will in most cases mean a certain loss to benthic predation so the processes will have a direct effect on the reproduction success. Another issue due to reduced buoyancy of eggs would be in areas with hypoxic bottom water where survivability of eggs would drastically be reduced. Studies on marine invertebrates of suspended sediments in the water mass show effects in concentrations down to ranges between 10 and 25 mg/l, higher compared with the levels of suspended sediment measured in the KNP (Larsson *et al.*, 2013; Tjensvoll *et al.*, 2013; Kutti *et al.*, 2015). However, sensitivity for larvae towards suspended material seems to be at lower concentrations compared with the adult individuals. Larsson *et al.* (2013) noticed a reduced survival for larvae from the cold-water coral *L. pertusa* after 5 days' exposure of levels with 5 mg/l.

In summary, we show that the background turbidity is elevated at depths of trawling and that much of the observed turbidity comes from fine particles, typical of silt–mud seafloor origin that remain suspended for days. The prevailing currents in the trench are slow, and water exchange of the trench in the MPA is limited, leading to prolonged periods of elevated turbidity. However, wind induced resuspension was also shown to generate events of elevated

turbidity probably due to lateral transport of particles resuspended in nearby shallower areas. Sediment particle levels in the trawl plumes may reach levels assessed to be harmful to marine organisms. However, mixing leads within hours to dilution of the plumes and thus lower turbidity and suspended particle concentration. The results provide useful input to conservation management considering the impact of trawling on the seafloor with regard to bottom trawling and advection of suspended sediment. The results are especially relevant for low energy areas, where there is little wind induced resuspension and little or moderate tides. This applies to many deeper shelf areas, where the bottom sediments typically consist of slowly sinking fine silt and clay particles. More energetic areas, affected by wind or tides, typically have bottom sediments consisting of coarser particles. This applies e.g. to the North Sea, which is shallow and has high tidal amplitudes.

## Acknowledgements

We thank the crews of R/V Nereus and R/V Skagerak for their professionalism and support during our expeditions. We thank Lars Arneberg, Bengt Liljebldh, Clara Calander, and Josefina Algotsson for help during parts of our surveys. This research was funded through County Administration Board of Västra Götalands Län to T.L., M.S., A.W., and P.N., and through the EU-FP7 project BENTHIS (grant 693 agreement number 312088) to M.S.

## References

- Agrawal, Y., and Pottsmith, H. 2000. Instruments for particle size and settling velocity observations in sediment transport. *Marine Geology*, 168: 89–114.
- Allredge, A. L., and Gotschalk, C. 1988. In situ settling behavior of marine snow. *Limnology and Oceanography*, 33: 339–351.
- Aure, J., and Saetre, R. 1981. Wind effects on the Skagerrak outflow in the Norwegian Coastal Current. *In Norwegian Coastal Current Symposium*, Geilo, pp. 263–293. Ed. by R. Saetre and J. Aure, September 1980. University of Bergen, Bergen, Norway.
- Bergström, U., Sköld, M., Wennhage, H., and Wikström, A. 2016. Ekologiska effekter av fiskefria områden i Sveriges kust- och havsområden. Aqua reports 2016: 20. Department of Aquatic Resources, Swedish University of Agriculture, Öregrund, Sweden, p. 207 (In Swedish).
- Bradshaw, C., Tjensvoll, I., Sköld, M., Allan, I., Molvaer, J., Magnusson, J., Naes, K., and Nilsson, H. 2012. Bottom trawling resuspends sediment and releases bioavailable contaminants in a polluted fjord. *Environmental Pollution*, 170: 232–241.
- Cato, I. 2006. Environmental quality and trends in sediment and biota along the Bohus Coast in 2000/2001 – a report from seven trend-monitoring programmes, Reports and bulletins. Geological Survey of Sweden. In Swedish, with key information in English, 122 pp. ISBN 91-7158-702-0; ISSN 0349-2176.
- Churchill, J. H. 1989. The effect of commercial trawling on sediment resuspension and transport over the Middle Atlantic Bight continental shelf. *Continental Shelf Research*, 9: 841–865.
- Churchill, J., Wirick, C., Flagg, C., and Pietrafesa, L. 1994. Sediment resuspension over the continental shelf east of the Delmarva Peninsula. *Deep Sea Research Part II: Topical Studies in Oceanography*, 41: 341–363.
- Danielsson, A., Jönsson, A., and Rahm, L. 2007. Resuspension patterns in the Baltic proper. *Journal of Sea Research*, 57: 257–269.
- Depestele, J., Ivanović, A., Degrendele, K., Esmaeili, M., Polet, H., Roche, M., Summerbell, K. *et al.* 2016. Measuring and assessing the physical impact of beam trawling. *ICES Journal of Marine Science*, 73: i15–i26.
- Diesing, M., Stephens, D., and Aldridge, J. 2013. A proposed method for assessing the extent of the seabed significantly affected by

- demersal fishing in the Greater North Sea. *ICES Journal of Marine Science*, 70: 1085–1096.
- Dounas, C., Davies, I., Triantafyllou, G., Koulouri, P., Petihakis, G., Arvanitidis, C., Sourlatzis, G. *et al.* 2007. Large-scale impacts of bottom trawling on shelf primary productivity. *Continental Shelf Research*, 27: 2198–2210.
- Floderus, S., and Pihl, L. 1990. Resuspension in the Kattegat: Impact of variation in wind climate and fishery. *Estuarine, Coastal and Shelf Science*, 31: 487–498.
- Gerritsen, H., and Lordan, C. 2011. Integrating vessel monitoring systems (VMS) data with daily catch data from logbooks to explore the spatial distribution of catch and effort at high resolution. *ICES Journal of Marine Science*, 68: 245–252.
- Gilmour, J. 1999. Experimental investigation into the effects of suspended sediment on fertilisation, larval survival and settlement in a scleractinian coral. *Marine Biology*, 135: 451–462.
- Gustafsson, B., and Stigebrandt, A. 1996. Dynamics of the fresh water influenced surface layers in the Skagerrak. *Journal of Sea Research*, 35: 39–53.
- Hall, S. J. 1994. Physical disturbance and marine benthic communities: life in unconsolidated sediments. *Oceanography and Marine Biology: An Annual Review*, 32, 179–239.
- Heywood, K., Scrope-Howe, S., and Barton, E. 1991. Estimation of zooplankton abundance from shipborne ADCP backscatter. *Deep Sea Research Part A. Oceanographic Research Papers*, 38: 677–691.
- Hongve, D., and Åkesson, G. 1998. Comparison of nephelometric turbidity measurements using wavelengths 400–600 and 860 nm. *Water Research*, 32: 3143–3145.
- Humborstad, O., Jørgensen, T., and Grotmol, S. 2006. Exposure of cod *Gadus morhua* to resuspended sediment: an experimental study of the impact of bottom trawling. *Marine Ecology Progress Series*, 309: 247–254.
- Johnston, D. D., and Wildish, J. D. 1982. Effects of suspended Sediment on feeding by larval herring (*Clupea harengus harengus* L.). *Bulletin of Environmental Contaminants and Toxicology*, 29: 261–267.
- Klingberg, F. 2015. Beskrivning till den maringeologiska kartan Väderöarna –Strömstad. Sveriges Geologiska Undersökning. SGU report K 511. ISSN 1652-8336, ISBN 978-91-7403-317-5 (In Swedish).
- Kundu, P. K., and Cohen, I. M., 2002. *Fluid Mechanics*, 2nd ed. Academic Press: San Diego, CA, USA. 730 pp.
- Kutti, T., Bannister, R. J., Fosså, J. H., Krogness, C. M., Tjensvoll, I., and Søvik, G. 2015. Metabolic responses of the deep-water sponge *Geodia barretti* to suspended bottom sediment, simulated mine tailings and drill cuttings. *Journal of Experimental Marine Biology and Ecology*, 473: 64–72.
- Larsson, A. I., Oevelen, D. V., Purser, A., and Thomsen, L. 2013. Tolerance to long-term exposure of suspended benthic sediments and drill cuttings in the cold water coral *Lophelia pertusa*. *Marine Pollution Bulletin*, 70: 176–188.
- Liljebladh, B., and Thomasson, M. 2001. Krill behaviour as recorded by acoustic doppler current profilers in the Gullmarsfjord. *Journal of Marine Systems*, 27: 301–313.
- Lynch, D. R., Greenberg, D. A., Bilgili, A., McGillicuddy, J., Dennis, J., and Manning, J. P. 2015. *Particles in the Coastal Ocean: Theory and Applications*. 1st ed. Cambridge University Press, New York, NY.
- Martín, J., Puig, P., Palanques, A., and Ribó, M. 2014a. Trawling-induced daily sediment resuspension in the flank of a Mediterranean submarine canyon. *Deep Sea Research Part II: Topical Studies in Oceanography*, 104: 174–183.
- Martín, J., Puig, P., Masqué, P., Palanques, A., Sánchez-Gómez, A., and Vopel, K. C. 2014b. Impact of bottom trawling on deep-sea sediment properties along the flanks of a submarine canyon. *PLoS One*, 9: e104536.
- Molvær, J., Magnusson, J., Næs, K., and Schaanning, M. 2012. Sedimentoppvirvling under reketråling i Eidangerfjorden juni 2008, NIVA-rapport 6282, Norsk institutt for vannforskning. In Norwegian.
- Moore, K., Wetzel, R., and Orth, R. 1997. Seasonal pulses of turbidity and their relations to eelgrass survival in an estuary. *Journal of Experimental Marine Biology and Ecology*, 215: 115–134.
- Newton, P., and Liss, P. 1990. Particles in the oceans (and other natural waters). *Science Progress*, 1933: 91–114.
- Oberle, F. K. J., Storlazzi, C. D., and Hanebuth, T. J. J. 2016. What a drag: Quantifying the global impact of chronic bottom trawling on continental shelf sediment. *Journal of Marine Systems*, 159: 109–119.
- O’Neill, F., and Summerbell, K. 2011. The mobilisation of sediment by demersal otter trawls. *Marine Pollution Bulletin*, 62: 1088–1097.
- Palanques, A., Martín, J., Puig, P., Guillén, J., Company, J. B., and Sardà, F. 2006. Evidence of sediment gravity flows induced by trawling in the Palamos (Fonera) submarine canyon (northwestern Mediterranean). *Deep-Sea Research I*, 53: 201–214.
- Paradis, S., Puig, P., Masqué, P., Juan-Díaz, X., Martín, J., and Palanques, A. 2017. Bottom-trawling along submarine canyons impacts deep sedimentary regimes. *Scientific Reports*, 7: 43332.
- Puig, P., Canals, M., Company, J. B., Martín, J., Amblas, D., Lastras, G. *et al.* 2012. Ploughing the deep sea floor. *Nature*, 489: 286–289.
- Pusceddu, A., Bianchelli, S., Martín, J., Puig, P., Palanques, A., Masqué, P., and Danovaro, R. 2014. Chronic and intensive bottom trawling impairs deep-sea bio-diversity and ecosystem functioning. *Proceedings of the National Academy of Sciences of the United States of America*, 111: 8861–8866.
- Rippeth, T., and Simpson, J. 1998. Diurnal signals in vertical motions on the Hebridean Shelf. *Limnology and Oceanography*, 43: 1690–1696.
- Rodhe, J. 1998. The Baltic and North Seas: a process-oriented review of the physical oceanography. *The Sea*, 11: 699–732.
- Sherwood, C., Butman, B., Cacchione, D., Drake, D., Gross, T., Sternberg, R., Wiberg, P., and Williams, A., III 1994. Sediment-transport events on the northern California continental shelf during the 1990–1991 STRESS experiment. *Continental Shelf Research*, 14: 1063–1099.
- SMHI. 2017. Sea ice. Webpage. Swedish Meteorological and Hydrological Institute. [Mismatch] <https://www.smhi.se/klimat/data/oceanografi/havsis> (last accessed 15 September 2017).
- SwAM, 2004. Fiske i Skagerrak, Kattegatt och Östersjön, Technical report. FIFS 2004: 36, Swedish Agency for Marine and Water Management. Updated 2017. In Swedish.
- Svansson, A. 1975. Physical and chemical oceanography of the Skagerrak and the Kattegat: I. Open sea conditions. Technical report. Fishery Board of Sweden.
- Tjensvoll, I. 2014. Sediment resuspension: Impacts and extent of human disturbances, PhD thesis, Stockholm University, Stockholm, Sweden.
- Tjensvoll, I., Kutti, T., Fosså, J. H., and Bannister, R. J. 2013. Rapid respiratory responses of the deep-water sponge *Geodia barretti* exposed to suspended sediments. *Aquatic Biology*, 19: 65–73.
- Wentworth, C. 1922. A scale of grade and class terms for clastic sediments. *The Journal of Geology*, 30: 377–392.
- Westerberg, H., Rönnbäck, P., and Frimansson, H. 1996. Effects of suspended sediments on cod eggs and larvae and on the behaviour of adult herring and cod. *ICES Council Meeting Papers*. ICES-CM-1996/E: 26. ICES Council Meeting of the International Council for the Exploration of the Sea, 27 September–4 October 1996. Reykjavik (Iceland).

Handling editor: Michel Kaiser